Accepted Manuscript

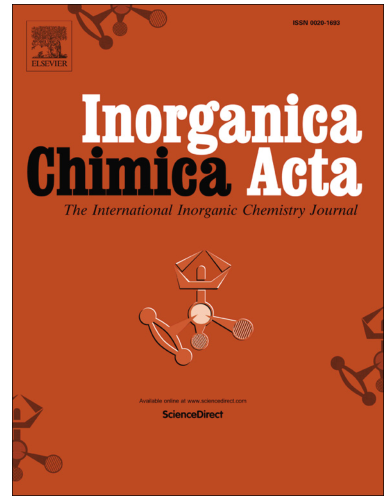

Bio-Inspired Oxidation Chemistry of a Cu(II)-Fluoride Cryptate with C3-Symmetry

Laura Chaloner, Xavier Ottenwaelder

PII: S0020-1693(17)31216-1
DOI: https://doi.org/10.1016/j.ica.2017.10.027
Reference: ICA 17954

To appear in: *Inorganica Chimica Acta*

Received Date: 1 August 2017
Revised Date: 20 October 2017
Accepted Date: 24 October 2017

Please cite this article as: L. Chaloner, X. Ottenwaelder, Bio-Inspired Oxidation Chemistry of a Cu(II)-Fluoride Cryptate with C3-Symmetry, *Inorganica Chimica Acta* (2017), doi: https://doi.org/10.1016/j.ica.2017.10.027

Bio-Inspired Oxidation Chemistry of a Cu(II)-Fluoride Cryptate with C3-Symmetry

Laura Chaloner and Xavier Ottenwaelder*

Department of Chemistry and Biochemistry, Concordia University, 7141 Sherbrooke Street West, Montreal, H4B 1R6, Canada.

Abstract. Three copper complexes with an *N*-methylated cryptand, **LTEA**, bearing a tris(2-aminoethylamine moiety have been synthesized and compared. Two copper(II)-chloride complexes, [**LTEA**CuCl](SbF_6)(MeOH) and [**LTEA**$CuCl_2$](MeCN) were characterized in solution and solid state by UV/Vis and X-ray crystallography. Both had square-based geometries with C_1-symmetry and no encapsulation of the chloride ion. A Cu(II)-fluoride complex, in which the ligand is protonated, [**LTEA**HCuF]$(BF_4)_2(MeCN)_{0.5}$, adopted C_3-symmetry with complete encapsulation of the coordination sphere as characterized by UV/Vis, EPR and X-ray crystallography. Reactivity of the complexes with H_2O_2/Et_3N was explored using UV/Vis and CSI-MS. Only the fluoride complex was found to form a Cu(II)-hydroperoxo intermediate.

Keywords: copper, fluoride, hydroperoxide, cryptand, oxidation, oxygen-atom transfer

1 Introduction

Biomimetic studies of Cu-F bonds are important because of the ability of fluoride ions to inhibit oxidative metallo-enzyme activity.[1] Tyrosinase, an ubiquitous oxygenase enzyme,[2] is competitively inhibited by fluoride ions that coordinate to the dinuclear copper(II) active site. The inhibition is regulated by physiological conditions (low pH) and conformational changes in the protein backbone.[3]

Supramolecular structures such as macrocycles, cavitands and cryptands have been used to mimic features of protein backbones, especially their hydrophobicity or capacity for weak interactions. This led to interesting applications in anion sensing[4] or biomimetic coordination chemistry,[5, 6] including the selective recognition of aqueous fluoride anion by an encapsulated Cu(II) center.[7] Cryptands are especially useful in studying highly reactive biomimetic intermediates, like those in oxygenase enzymes, because they have the ability to protect the metal center through second coordination sphere features while simplifying the overall chemistry and reaction products. We have applied this concept to the characterization of Cu-based oxidative reactions within coordinating cryptands.[8, 9] Herein, we provide the first study that explores the biomimetic relationship between Cu-F cryptates and the formation of Cu/O_2 intermediates.

Tren (tris-(2-aminoethyl)amine)-based coordinating cryptands are popular because of their high yielding syntheses when condensing with tris-aldehydes and because of their ability to form well-defined complexes with transition metals.[10-12] They have been used in applications such as ion sequestering and sensing[13-15] and host-guest chemistry.[16] They are, however, limited in the area of biomimetic oxidation chemistry because in the presence of metals, the secondary amines are easily oxidized to form imines complicating the reactions with several by-products.[17-19] *N*-Methylation is an easy solution to reduce side reactions under oxidative conditions but the additional steric constraint on the cryptand prevents encapsulation of transition metals with anionic hosts,[20, 21] with encapsulation defined here as coordination of the five donor atoms of Tren. Using cryptand **LTEA** (Figure 1A), we here present Cu(II)-halide cryptates and their reactivity with basic hydrogen peroxide (H_2O_2/Et_3N).

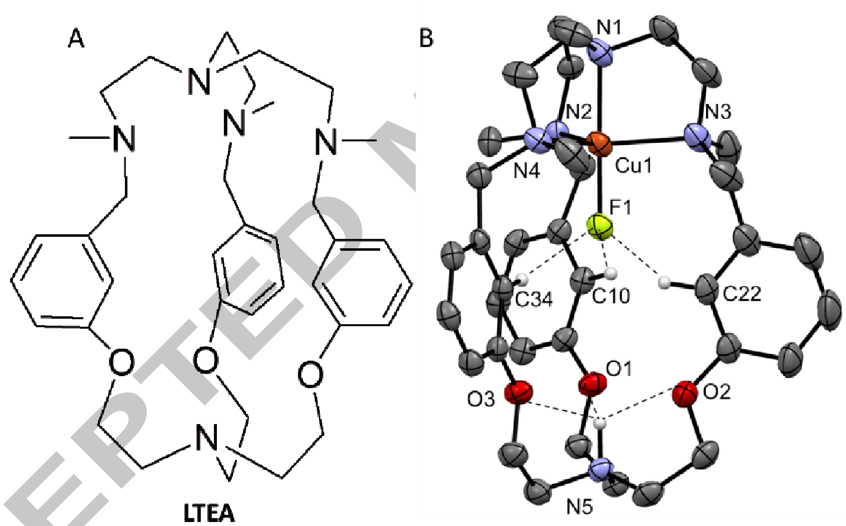

Figure 1. A) Cryptand **LTEA** B) ORTEP representation at 50% thermal ellipsoid probability of [**LTEA**HCuF]$(BF_4)_2(MeCN)_{0.5}$. Hydrogen atoms, non-coordinating anions and solvent molecules have been omitted for clarity except for H5N, H10, H22 and H34. Dashed lines represent intramolecular hydrogen bonds.

2 Results and Discussion

A protonated copper(II) fluoride complex is formed by mixing copper(II)-tetrafluoroborate with **LTEA** in acetonitrile followed by slow diffusion in ether. ESI-MS reveals that the complex has acquired a fluoride ion from the BF_4^- anion, a well-documented phenomenon.[22] The X-ray structure of [**LTEA**HCuF]$(BF_4)_2(MeCN)_{0.5}$ reveals that the copper center is entirely encapsulated by the cryptand despite *N*-methylation of the Tren moiety (Figure 1B, Table 1). The overall C_3 symmetry of the complex is driven by intramolecular hydrogen bonding. A trifurcate hydrogen bond between the protonated amine and the electronegative oxygen atoms is observed at the base of the tris(ethanolamine) moiety (O···H = 2.17-2.38 Å, r_{vdW}: H, 1.20 O, 1.52 Å). The metal center has trigonal-bipyramidal geometry with a fluoride ion in the axial positions (τ = 0.98).[23] The electronegative fluoride is stabilized by weak but significant hydrogen bonds with the aromatic rings of the ligand (H···F = 2.188-2.228 Å, r_{vdW}: H, 1.20 F, 1.47 Å).[24] The three aromatic rings are all slightly rotated, creating C-H···F angles from 130 to 136° (Table 2). The Cu(II)-F bond of 1.824(1) Å is among the shortest ever reported, with the ten shortest Cu-F bonds ranging from 1.804 to 1.862 Å.[25][7, 26-33]

Table 1. Summary of Crystallographic Data.

		[**LTEA**HCuF]$(BF_4)_2(MeCN)_{0.5}$	[**LTEA**CuCl](SbF_6)(MeOH)	[**LTEA**$CuCl_2$](MeCN)
CCDC deposition number		1566053	1566054	1566055
Formula		$C_{37}H_{53.5}B_2CuF_9N_{5.5}O_3$	$C_{37}H_{55}Cl_1CuF_6N_5O_4Sb$	$C_{38}H_{54}Cl_2CuN_6O_3$
M_w(g/mol); F(000)		879.51; 1832	968.60; 1980	777.31; 1644
T(K); wavelength		150; 1.54178	150; 1.54178	150; 1.54178
Crystal System		Monoclinic	Monoclinic	Monoclinic
Space Group		$P\ 2_1/n$	$P\ 2_1/c$	$P\ 2_1/n$
Unit Cell:	a (Å)	21.6285(7)	12.0729(11)	16.6170(5)
	b (Å)	12.1322(4)	11.5223(15)	12.5970(3)
	c (Å)	16.8581(6)	28.087(3)	20.2250(6)
	α (˚)	90	90	90
	β (˚)	111.381(2)	98.314(4)	90.935
	γ (˚)	90	90	90
V ($Å^3$)		4233.2(2)	4119.1(2)	3866.1(7)
Z; $d_{calcd.}$ (g/cm^3)		4; 1.380	4; 1.562	4; 1.335
Θ range (˚); completeness		3.14- 59.557; 0.991	2.19- 68.57; 0.979	3.18– 70.80; 0.985
Collected reflections; R_σ		53624; 0.0285	57632; 0.0338	50926; 0.0892
Unique reflections; R_{int}		6152; 0.0619	7438; 0.0554	7330; 0.1503
μ (mm^{-1}); Abs. Corr		1.442; Multi-Scan	7.054; Multi-Scan	2.416; Multi-Scan
R1(F); wR(F^2) [I> 2σ(*I*)]		0.0370; 0.0836	0.0647; 0.1719	0.0561; 0.1140
R1(F); wR(F^2) (all data)		0.0529; 0.911	0.0724; 0.1798	0.1021; 0.1397
GoF (F^2)		1.038	1.063	1.048
Residual electron density ($e^-/Å^3$)		0.374	0.927	0.535

Table 2. Hydrogen bond lengths and angles for [**LTEA**HCuF]$(BF_4)_2(MeCN)_{0.5}$

D-H···A	D-H (Å)	H···A (Å)	D···A (Å)	∡D-H···A (°)
C10-H10··· F1	0.950	2.194	2.904(3)	130.7
C22-H22··· F1	0.950	2.228	2.944(3)	131.5
C34-H34··· F1	0.949	2.188	2.951(3)	136.6
N5-H5N··· O1	1.04(2)	2.38(2)	2.820(3)	104(2)
N5-H5N··· O2	1.04(2)	2.21(2)	2.730(3)	109(2)
N5-H5N··· O3	1.04(2)	2.17(2)	2.734(3)	112(2)

In parallel to the encapsulated Cu(II)-fluoride complex, we isolated two Cu(II)-chloride complexes, [**LTEA**CuCl](SbF_6)(MeOH) and [**LTEA**$CuCl_2$](MeCN), which, however, do not adopt an overall C_3 symmetry (Figure 2). The Cu(II) ion of [**LTEA**CuCl](SbF_6)(MeOH) has a distorted square-planar geometry (τ = 0.40) and [**LTEA**$CuCl_2$](MeCN) has a square-pyramidal geometry (τ = 0.13). In both complexes, three of the equatorial positions are occupied by amines from the Tren moiety (N1, N2 and N3) and the fourth equatorial position is occupied by a chloride ion (Cl1). The fourth nitrogen (N4) in the Tren moiety and is completely uncoordinated. [**LTEA**$CuCl_2$](MeCN) is distinguished by a second chloride ion (Cl2) in the axial position with the copper ion lying slightly above the N1, N2, N3, Cl1 plane, displaced towards Cl2. These *N*-Methylated cryptands are not encapsulating because of the steric influence of the methyl groups and the increased rigidity of the cryptand.[21] If the macrobicyclic tension of the cryptand is removed, the metal center adopts a TBP geometry, as observed by Suzuki and coworkers in the Cu(II)-chloride complex with tris(*N*-benzyl-*N*-methylaminoethyl)amine.[34] Alternatively, removing the methyl groups from the cryptand, as studied by Bharadwaj and Chand, allows for encapsulation of a Cu(II)-X metal center (X = N_3^-, CN^-, SCN^-) in TBP geometry.[35, 36] The two copper chloride structures in this work show that the steric influence from the cryptand and methyl groups prevent encapsulation of the metal-chloride center and that [**LTEA**HCuF]$(BF_4)_2$ is a truly unique with its C_3 symmetry.

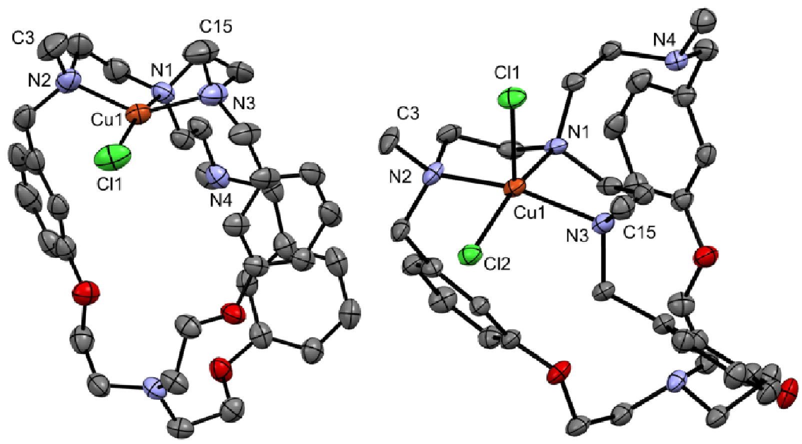

Figure 2. ORTEP representation at 50% thermal ellipsoid probability of [**LTEA**CuCl](SbF_6)(MeOH) (left) and [**LTEA**$CuCl_2$](MeCN) (right). Hydrogen atoms, non-coordinating anions and solvent molecules have been omitted for clarity.

Solution studies were carried out to confirm the conservation of the solid-state geometry in solution. The UV/Vis spectrum of [**LTEA**HCuF](BF_4)$_2$ in MeCN has d→d transitions at 690 nm (ε = 180 M^{-1} cm^{-1}) and 860 nm (ε = 168 M^{-1} cm^{-1}) that are traditionally associated with TBP complexes (Figure 3A).[37-39] Its EPR spectrum is best fitted to a mononuclear Cu(II) complex (S = 1/2) with a $d(z^2)^1$ ground state where $g_{\parallel}$ = 2.065, $A_{\parallel}$ = 68 G, $g_{\perp}$ = 2.221 and $A_{\perp}$ = 82 G (Figure 4). The ordering of $g_{\perp} > g_{\parallel}$ confirms the TBP geometry in solution. The UV/Vis spectra of the two chloride complexes show retention of a square-based geometry in solution, confirmed by the two characteristic transitions at 580 and 770 nm associated with square-pyramidal or square-planar geometries (Figure 5).[37, 40]

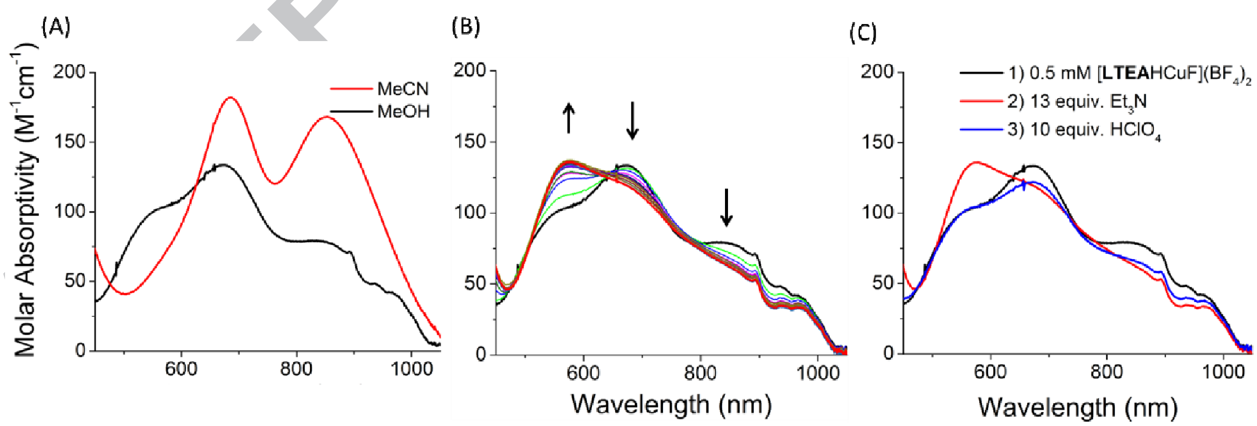

Figure 3. UV/Vis spectra (A) 0.5 mM [**LTEA**HCuF](BF_4)$_2$ in MeCN and MeOH (B) Serial additions of 1 equiv. of Et_3N (Total = 10 equiv.) to 0.5 mM [**LTEA**HCuF](BF_4)$_2$ in MeOH. The black arrows show the trend in spectral changes after addition of the base. (C) 1) [**LTEA**HCuF](BF_4)$_2$ in MeOH followed by sequential addition of 2) Et_3N and 3) $HClO_4$

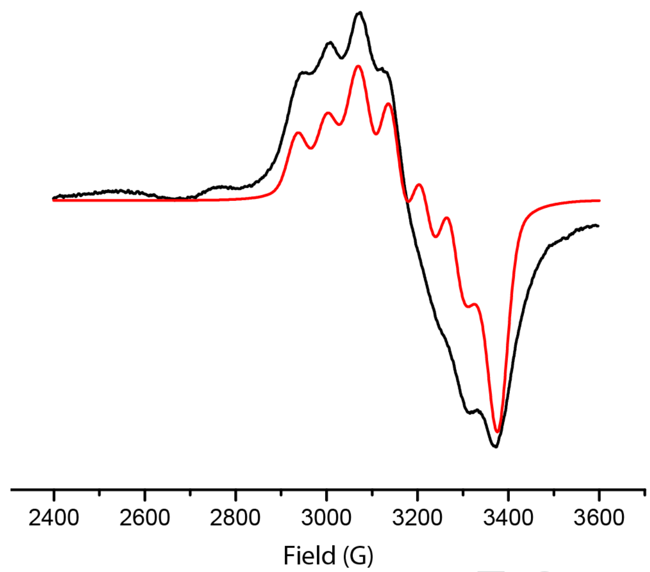

Figure 4. EPR spectra (black) of [**LTEA**HCuF]$(BF_4)_2(MeCN)_{0.5}$ in acetonitrile at 100K, with simulation (red) using parameters given in the text.

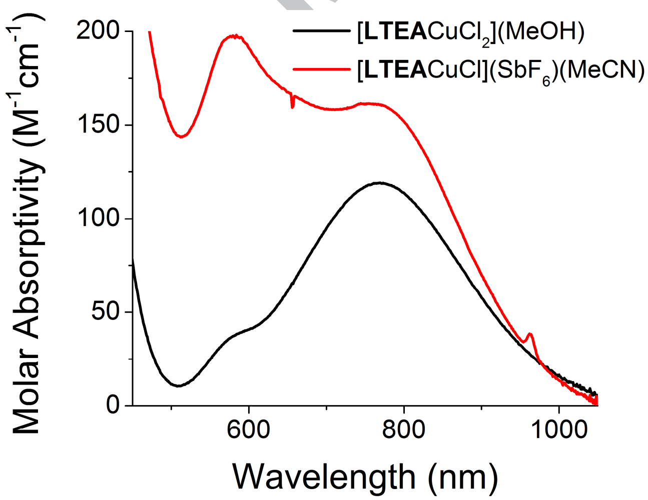

Figure 5. UV/Vis spectra Red: 0.5 mM [**LTEA**$CuCl_2$](MeOH) dissolved in CH_2Cl_2 and Black: 0.5 mM [**LTEA**CuCl](SbF_6)(MeCN) dissolved in CH_2Cl_2.

The geometry of [**LTEA**HCuF]$(BF_4)_2$ is influenced by solvent and the protonation state of the cryptand. The geometry in MeCN is TBP but in methanolic solution the geometry changes with the appearance of a new transition with a maximum at 555 nm (ε = 100 M^{-1} cm^{-1}) (Figure 3A). The complex in methanol shows a dependence on base (Et_3N) indicating that the cryptand is still protonated and that the pKa of the protonated ligand is very close to that of Et_3NH^+ (Figure 3B). This addition of base leads to a complex with a square-based geometry evidenced by absorption bands at 580 nm (ε = 135 $M^{-1}cm^{-1}$) and 672 (ε = 120 M^{-1} cm^{-1}).[37, 40] The protonated cryptate can be regenerated by addition of an acid (Figure 3C). Attempts to induce C_3 symmetry by adding acids to the chloride complexes failed and the reason is likely a combination of the increased ionic radius of the chloride ion and formation of weaker intramolecular hydrogen bonds. H···Cl bond distances are consistently 0.5 Å longer then H···F bond distances.[41] To accommodate a chloride ion, the cryptand would have to severely expand the cavity in the equatorial direction and compress axially (increasing the CH···O bond length) and further rotate the aromatic rings (weakening the Cl···H hydrogen bond).

Biomimetic oxidative studies were investigated by reacting the [**LTEA**$CuCl_2$] and [**LTEA**HCuF]$(BF_4)_2$ complexes with H_2O_2/Et_3N at -30 °C and following with UV/Vis spectroscopy. No change was observed with [**LTEA**CuCl]Cl. When [**LTEA**HCuF]$(BF_4)_2$ was reacted with H_2O_2/Et_3N, a color change from turquoise to green was observed. A Cu(II)-hydroperoxo intermediate was identified by the growth of a characteristic LMCT band at 388 nm (Figure 6).[42] The intermediate had the same UV/Vis spectrum as a previously characterized Cu(II)-hydroperoxo species starting from a Cu(II)-acetate complex with the **LTEA**.[8] This suggests that the two intermediates are the same, with a square-based geometry, despite different anions in the starting complexes.

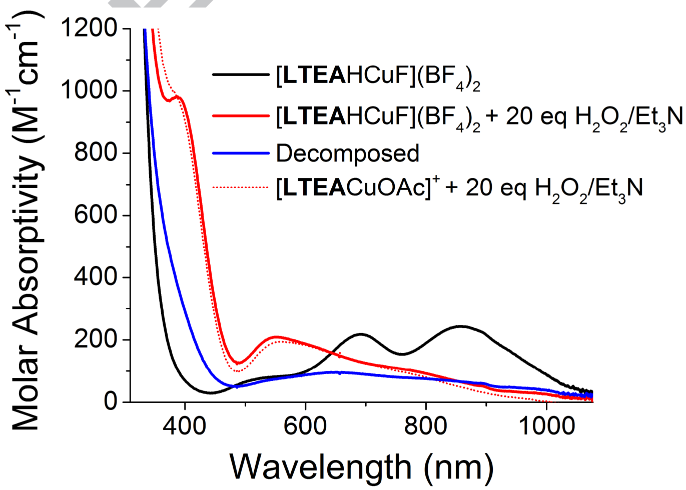

Figure 6. UV/Vis spectra of Black: 0.5 mM [**LTEA**HCuF]$(BF_4)_2$ at -30°C Red: Addition of 20 eq H_2O_2/Et_3N, Blue: Decomposed after 35 min and Dotted Red: **LTEA**CuOAc + 20 eq H_2O_2/Et_3N at -30°C.[8]

The reaction of [**LTEA**HCuF]$(BF_4)_2$ with 15 equiv. of H_2O_2/Et_3N was followed using a continuous-flow mixing setup directed into a Cryospray Ionization Mass Spectrometer (CSI-MS). Before mixing, the spectrum consists mostly of [**LTEA**]H^+ (m/z = 602.40), [**LTEA**CuF]$^+$ (m/z = 683.32) and a small signal from [**LTEA**Cu]$^+$ m/z = 664.32 (Figure 7). The spectrum also contains a small amount of [**LTEA**CuOAc]$^+$ m/z = 723.33, an unavoidable contaminant in this instrument. The MS after reacting with H_2O_2/Et_3N, shows the same m/z signals as the reaction starting solely from [**LTEA**CuOAc]$^+$ (with the exception of [**LTEA**CuF]$^+$ and [(**LTEA**+O) CuF]$^+$). The similarity in the two spectra further supports similar reaction pathways despite different starting complexes. The most intense signal in the reaction of [**LTEA**CuOAc]$^+$ with H_2O_2/Et_3N is [(**LTEA**+O)CuOAc]$^+$ whereas the most intense signal from [**LTEA**HCuF]$(BF_4)_2$ with H_2O_2/Et_3N is m/z = 697, (identified as [(**LTEA**+O)CuOH]$^+$) and not [(**LTEA**+O)CuF]$^+$. This difference suggests a less favorable binding of the fluoride anion to the copper center with (**LTEA+O**) compared with the acetate anion.

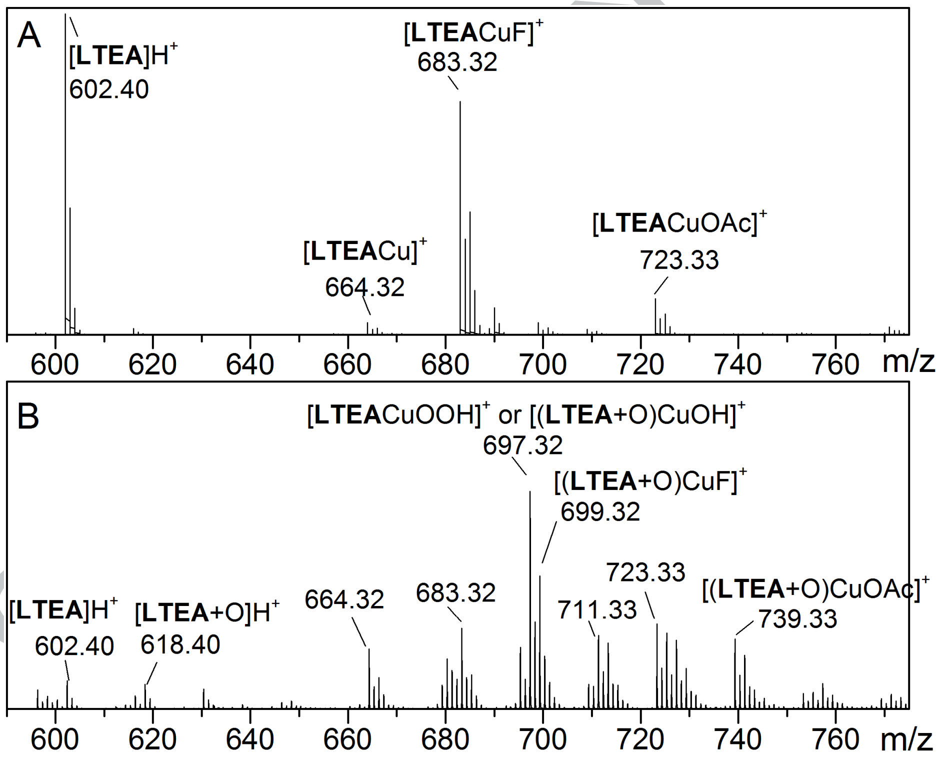

Figure 7. CSI-MS of [**LTEA**HCuF]$(BF_4)_2$ + 15 equiv. H_2O_2/Et_3N in methanol mixed with a continuous-flow methods at RT. The spectra were recorded A: before mixing and B: after mixing. Impurities from Cu(II)-acetate complexes are present.

The lack of reactivity of the chloride complex compared with the fluoride complex can be explained by the Cu-halide bond strength and hard/soft characteristics. The fluoride anion forms a weaker σ-bond with copper and has greater π-donation which has a more destabilizing effect due to the filled d orbitals of copper.[43] While the hard characteristic of the Cu(II) ion is unselective to halide ions the cryptand influences this property, creating a softer Cu(II) center that more favorably binds chloride ions.[43]

Although mononuclear, the reactivity of [**LTEA**HCuF]$(BF_4)_2$ has similarities to the dinuclear biological system tyrosinase. Tyrosinase systems are inhibited by bridged halides at low pH but undergo reactions at high pH.[1] This behavior is paralleled by the copper fluoride cryptate whereby addition of a base to the protonated cryptand changes the environment of the metal center. The geometry change triggered by the deprotonation of the cryptand is a behavior that is reminiscent of a conformational change observed in many enzymes.[44] Under basic conditions the formation of a Cu(II)-hydroperoxo intermediate is possible. Current investigations are underway to determine if the pH change triggers release of the fluoride anion, as well as investigations into the reactivity of the hydroperoxo intermediate.

3 Conclusion

In conclusion, Cu(II)-halide cryptate complexes were formed and characterized. C_3 symmetry was observed in the Cu(II)-fluoride cryptate, despite *N*-methylation, while C_1 symmetry was observed in the Cu(II)-chloride complexes. The difference in symmetry was attributed to the stronger intramolecular hydrogen bonding and smaller ionic radius with the fluoride anion. The Cu(II)-fluoride complex when reacted with basic hydrogen peroxide was capable of forming a bio-relevant Cu(II)-hydroperoxo intermediate. In comparison, a Cu(II)-chloride complex was unable to form the same intermediate and the difference in reactivity was rationalized by the different bond strengths and stability of Cu(II)-halide complexes.

4 Experimental Section

4.1 General

All materials were used as received from commercial sources. The synthesis of **LTEA** was reported elsewhere.[8] ESI-MS spectra were measured using direct injection on Micromass Quattro LC at Concordia's Center for Biological Applications of Mass Spectrometry. The CSI-MS was recorded on a Bruker Micro-TOF II equipped with a cold spray adapted at the Université de Montréal. The *m*/*z* data reported is based on ^{1}H, ^{12}C, ^{14}N, ^{16}O, ^{19}F, ^{35}Cl, ^{63}Cu. X-Ray crystallography was performed on the copper source of a Bruker APEX DUO. UV-Vis spectra were recorded on an Agilent 8453 spectrophotometer equipped with a Unisoku USP-203-A cryostat for temperatures down to –30°C. X-band EPR spectra were collected on a Bruker EMX Plus spectrometer controlled with Xenon software and equipped with a Bruker teslameter. A Bruker nitrogen-flow cryostat connected to a high-sensitivity resonant cavity was used for 100 K measurements. The EPR spectra were fit with Easyspin Fitting software.[45] X-ray crystallographic analysis was performed using the Cu-Kα microfocus source of a Bruker APEX-DUO diffractometer. The frames were integrated with the Bruker SAINT software package using a narrow-frame algorithm. Data were corrected for absorption effects using the multi-scan method (SADABS). The structures were solved by direct methods and refined using the Bruker APEX2 software Package (SHELXL instructions).[46] All non-hydrogen atoms were refined with anisotropic thermal parameters. Hydrogen atoms were generated in idealized positions, riding on the carrier atoms, with isotropic thermal parameters.

4.2 Synthesis

[LTEAHCuF]$(BF_4)_2(MeCN)_{0.5}$: To **LTEA** (15 mg, 25 µmol) suspended in 1 mL of acetonitrile was added copper(II) tetrafluoroborate (8.61 mg, 25 µmol) dissolved in 1 mL acetonitrile. The mixture was stirred for 10 minutes and a dark green solution evolved. The complex was isolated by precipitating with diethyl ether to afford 11.5 mg (50 %) of a turquoise powder. Single crystals suitable for X-ray diffraction were grown with slow diffusion of diethyl ether into a solution of the complex in acetonitrile at RT (Table 1). ESI-MS in MeCN: *m*/*z* = 683.

[LTEACuCl](SbF_6)(MeOH): To **LTEA** (10 mg, 20 µmol) suspended in 1 mL of methanol was added copper(II) chloride (3.4 mg, 20 µmol) dissolved in 1 mL of methanol. The mixture was stirred for 10 minutes and a dark green color formed. The solution was used as is or alternatively single crystals were grown by adding $NaSbF_6$ (5.2 mg, 20 µmol) to the solution and evaporating the solvent overnight. The dark turquoise/ green crystals were collected in 58 % yield (11 mg, 11 µmol) (Table 1). ESI-MS in MeOH: *m*/*z* = 699.

[LTEA$CuCl_2$](MeCN): To **LTEA** (12 mg, 20 µmol) suspended in 1 mL of acetonitrile was added copper(II) chloride (3.4 mg, 20 µmol) dissolved in 1 mL of acetonitrile. The mixture was stirred for 10 minutes. The solvent was left to evaporate slowly overnight resulting in pale green crystals in 77 % yield (12.2 mg, 15 µmol) (Table 1). ESI-MS in MeCN: *m*/*z* = 699.

4.3 Reactivity

To a 1 cm UV-vis cell equipped with a stir bar, filled with 1.8 mL of MeOH and cooled to -30°C was added 100 µL of a 10 mM stock solution of [**LTEA**HCuF]$(BF_4)_2$ in MeCN or [**LTEA**CuCl](Cl) in MeOH. To the solution was added 100 µL of a 200 mM stock solution of H_2O_2/Et_3N in MeOH.

A continuous flow set-up was used to mix a 10 mM solution of [**LTEA**HCuF]$(BF_4)_2$ in MeOH with 15 equivalents H_2O_2/Et_3N in MeOH. The final concentration was 3.33 mM in copper.

5 Supplementary Material

Crystallographic data (CCDC 1566053-1566055).

6 Acknowledgements

This work has been supported by Fonds de Recherche du Québec - Nature et Technologies (FRQNT), the Natural Sciences and Engineering Research Council of Canada (NSERC) and the Canadian Foundation for Innovation (CFI). We would like to thank Pr. Garry Hanan and Dr. Jingwei Luo for access to the CSI-MS at the Université de Montréal. We are grateful to Pr. Fabrice Thomas (Université Joseph Fourier) for help with EPR measurements.

7 References

[1] A.W.J.W. Tepper, L. Bubacco, G.W. Canters, Structural Basis and Mechanism of the Inhibition of the Type-3 Copper Protein Tyrosinase from Streptomyces antibioticusby Halide Ions, J. Biol. Chem., 277 (2002) 30436-30444.

[2] E.I. Solomon, D.E. Heppner, E.M. Johnston, J.W. Ginsbach, J. Cirera, M. Qayyum, M.T. Kieber-Emmons, C.H. Kjaergaard, R.G. Hadt, L. Tian, Copper Active Sites in Biology, Chem. Rev., 114 (2014) 3659-3853.

[3] R.L. Osborne, J.P. Klinman, Insights into the Proposed Copper–Oxygen Intermediates that Regulate the Mechanism of Reactions Catalyzed by Dopamine β-Monooxygenase, Peptidylglycine α-Hydroxylating Monooxygenase, and Tyramine β-Monooxygenase, Copper-Oxygen Chemistry, John Wiley & Sons, Inc.2011, pp. 1-22.

[4] M.J. Langton, C.J. Serpell, P.D. Beer, Anion Recognition in Water: Recent Advances from a Supramolecular and Macromolecular Perspective, Angew. Chem., Int. Ed., 55 (2016) 1974-1987.

[5] J.-N. Rebilly, B. Colasson, O. Bistri, D. Over, O. Reinaud, Biomimetic cavity-based metal complexes, Chem. Soc. Rev., 44 (2015) 467-489.

[6] N. Le Poul, Y. Le Mest, I. Jabin, O. Reinaud, Supramolecular Modeling of Mono-copper Enzyme Active Sites with Calix[6]arene-based Funnel Complexes, Acc. Chem. Res., 48 (2015) 2097-2106.

[7] A. Brugnara, F. Topic, K. Rissanen, A.d.l. Lande, B. Colasson, O. Reinaud, Selective recognition of fluoride anion in water by a copper(ii) center embedded in a hydrophobic cavity, Chem. Sci., 5 (2014) 3897-3904.

[8] L. Chaloner, M.S. Askari, A. Kutteh, S. Schindler, X. Ottenwaelder, Formation and Reactivity of a Biomimetic Hydroperoxocopper(II) Cryptate, Eur. J. Inorg. Chem., 2011 (2011) 4204-4211.

[9] L. Chaloner, A. Khomutovskaya, F. Thomas, X. Ottenwaelder, Supramolecular control of monooxygenase reactivity in a copper(ii) cryptate, Dalton Trans., 45 (2016) 11109-11119.

[10] B. Sarkar, P. Mukhopadhyay, P.K. Bharadwaj, Laterally non-symmetric aza-cryptands: synthesis, catalysis and derivatization to new receptors, Coord. Chem. Rev., 236 (2003) 1-13.

[11] K. Ziach, M. Ceborska, J. Jurczak, Toward dynamic combinatorial libraries of cryptands, Tetrahedron Lett., 52 (2011) 4452-4455.

[12] G. Alibrandi, V. Amendola, G. Bergamaschi, L. Fabbrizzi, M. Licchelli, Bistren cryptands and cryptates: versatile receptors for anion inclusion and recognition in water, Org. Biomol. Chem., 13 (2015) 3510-3524.

[13] V. Amendola, L. Fabbrizzi, C. Mangano, P. Pallavicini, A. Poggi, A. Taglietti, Anion recognition by dimetallic cryptates, Coord. Chem. Rev., 219–221 (2001) 821-837.

[14] S.O. Kang, J.M. Llinares, V.W. Day, K. Bowman-James, Cryptand-like anion receptors, Chem. Soc. Rev., 39 (2010) 3980-4003.

[15] L. Fabbrizzi, A. Poggi, Anion recognition by coordinative interactions: metal-amine complexes as receptors, Chem. Soc. Rev., 42 (2013) 1681-1699.

[16] K. Gloe, Macrocyclic Chemistry: Current Trends and Future Perspectives, Springer2005.

[17] G. Izzet, J. Zeitouny, H. Akdas-Killig, Y. Frapart, S.p. Ménage, B.n.d. Douziech, I. Jabin, Y. Le Mest, O. Reinaud, Dioxygen Activation at a Mononuclear Cu(I) Center Embedded in the Calix[6]arene-Tren Core, J. Am. Chem. Soc., 130 (2008) 9514-9523.

[18] M. Largeron, Protocols for the Catalytic Oxidation of Primary Amines to Imines, Eur. J. Org. Chem., 2013 (2013) 5225-5235.

[19] M. Schatz, M. Becker, O. Walter, G. Liehr, S. Schindler, Reactivity towards dioxygen of a copper(I) complex of tris(2-benzylaminoethyl)amine, Inorg. Chim. Acta, 324 (2001) 173-179.

[20] D. Meyerstein, Are M–N bonds indeed inherently weaker when N is a tertiary rather than a primary or secondary nitrogen atom?, Coord. Chem. Rev., 185–186 (1999) 141-147.

[21] S. Derossi, D.T. Farrell, C.J. Harding, V. McKee, J. Nelson, N-methylation of macrobicycles reduces encapsulation ability, Dalton Trans., DOI 10.1039/b617907j(2007) 1762-1772.

[22] A.J. Cresswell, S.G. Davies, P.M. Roberts, J.E. Thomson, Beyond the Balz–Schiemann Reaction: The Utility of Tetrafluoroborates and Boron Trifluoride as Nucleophilic Fluoride Sources, Chem. Rev., 115 (2014) 566-611.

[23] A.W. Addison, T.N. Rao, J. Reedijk, J. van Rijn, G.C. Verschoor, Synthesis, structure, and spectroscopic properties of copper(II) compounds containing nitrogen-sulphur donor ligands; the crystal and molecular structure of aqua[1,7-bis(N-methylbenzimidazol-2[prime or minute]-yl)-2,6-dithiaheptane]copper(II) perchlorate, Dalton Trans., DOI 10.1039/dt9840001349(1984) 1349-1356.

[24] J. Reedijk, Coordination chemistry beyond Werner: interplay between hydrogen bonding and coordination, Chem. Soc. Rev., 42 (2013) 1776-1783.

[25] Cambridge Structural database, CSD (version 5.38, May 2017)

[26] T. Fujihara, T. Xu, K. Semba, J. Terao, Y. Tsuji, Copper-Catalyzed Hydrocarboxylation of Alkynes Using Carbon Dioxide and Hydrosilanes, Angew. Chem., Int. Ed., 50 (2011) 523-527.

[27] A. Almesaker, P. Gamez, J. Reedijk, J.L. Scott, L. Spiccia, S.J. Teat, Stabilisation of a very short Cu-F bond within the protected cavity of a copper(ii) compound from a tris(2-aminoethyl)amine derivative, Dalton Trans., DOI 10.1039/B902907A(2009) 4077-4080.

[28] P. Comba, C. Lopez de Laorden, H. Pritzkow, Tuning the Properties of Copper(II) Complexes with Tetra- and Pentadentate Bispidine (=3,7-Diazabicyclo[3.3.1]nonane) Ligands, Helv. Chim. Acta, 88 (2005) 647-664.

[29] R.R. Jacobson, Z. Tyeklar, K.D. Karlin, J. Zubieta, Fluoride as a terminal and bridging ligand for copper: isolation and x-ray crystallographic characterization of copper monomeric and dimeric complexes [CuII(TMPA)F]nn+ (n = 1 or 2; TMPA = tris[(2-pyridyl)methyl]amine), Inorg. Chem., 30 (1991) 2035-2040.

[30] D. Wiedemann, E. Świętek, W. Macyk, A. Grohmann, Copper(I) and Iron(II) Complexes of a Novel Tris(pyridyl)-ethane-Derived N4 Ligand: Aspects of Redox Behaviour and Bioinorganic Physicochemistry, Z. Anorg. Allg. Chem., 639 (2013) 1483-1490.

[31] G.A. van Albada, O. Roubeau, I. Mutikainen, U. Turpeinen, J. Reedijk, A unique methoxo- and fluoro-bridged triangular trinuclear Cu(ii) species linked in a lattice via mononuclear Cu(ii) units. Synthesis, X-ray structure and magnetism of [Cu4(2-aminopyrimidine)6([small mu]3-OCH3)2([small mu]-F)3(F)2](BF4), New J. Chem., 27 (2003) 1693-1697.

[32] J. Van Rijn, J. Reedijk, M. Dartmann, B. Krebs, Copper(I) and copper(II) compounds of a dinucleating, octadentate tetrakisbenzimidazole ligand. Crystal and molecular structures of three dihalogeno{1,8-bis[bis(1[prime or minute]-methylbenzimidazol-2[prime or minute]-ylmethyl)amino]-3,6-dioxaoctane}dicopper(II) bis(anion) compounds (halogen = F, Cl, or Br; anion = BF4, CF3SO3, or Cl), Dalton Trans., DOI 10.1039/DT9870002579(1987) 2579-2593.

[33] J. Emsley, M. Arif, P.A. Bates, M.B. Hursthouse, DIAQUABIS(1,3-DIAMINOPROPANE)COPPER(II) DIFLUORIDE - X-RAY STRUCTURE REVEALS SHORT HYDROGEN-BONDS BETWEEN LIGAND WATERS AND LATTICE FLUORIDES, Inorg. Chim. Acta, 154 (1988) 17-20.

[34] K. Komiyama, H. Furutachi, S. Nagatomo, A. Hashimoto, H. Hayashi, S. Fujinami, M. Suzuki, T. Kitagawa, Dioxygen Reactivity of Copper(I) Complexes with Tetradentate Tripodal Ligands Having Aliphatic Nitrogen Donors: Synthesis, Structures, and Properties of Peroxo and Superoxo Complexes, Bull. Chem. Soc. Jpn., 77 (2004) 59-72.

[35] D.K. Chand, P.K. Bharadwaj, Heteroditopic Cryptands of Tunable Cavity Size: Imposition of Distorted Geometry onto Copper(II) and Nickel(II) and Molecular Recognition of Water Molecules, Inorg. Chem., 37 (1998) 5050-5055.

[36] D.K. Chand, P.K. Bharadwaj, Synthesis of a Heteroditopic Cryptand Capable of Imposing a Distorted Coordination Geometry onto Cu(II): Crystal Structures of the Cryptand (L), [Cu(L)(CN)](picrate), and [Cu(L)(NCS)](picrate) and Spectroscopic Studies of the Cu(II) Complexes, Inorg. Chem., 35 (1996) 3380-3387.

[37] M. Duggan, N. Ray, B. Hathaway, G. Tomlinson, P. Brint, K. Pelin, Crystal structure and electronic properties of ammine[tris(2-aminoethyl)amine]copper(II) diperchlorate and potassium penta-amminecopper(II) tris(hexafluorophosphate), Dalton Trans., DOI 10.1039/dt9800001342(1980) 1342-1348.

[38] R. Barbucci, A. Mastroianni, M.J.M. Campbell, The effect of N-Alkylation on the properties of five-coordinate copper(II) complexes of tetra-amine ligands, Inorg. Chim. Acta, 27 (1978) 109-114.

[39] F. Thaler, C.D. Hubbard, F.W. Heinemann, R. van Eldik, S. Schindler, I. Fábián, A.M. Dittler-Klingemann, F.E. Hahn, C. Orvig, Structural, Spectroscopic, Thermodynamic and Kinetic Properties of Copper(II) Complexes with Tripodal Tetraamines, Inorg. Chem., 37 (1998) 4022-4029.

[40] G.A. McLachlan, G.D. Fallon, R.L. Martin, L. Spiccia, Synthesis, Structure and Properties of Five-Coordinate Copper(II) Complexes of Pentadentate Ligands with Pyridyl Pendant Arms, Inorg. Chem., 34 (1995) 254-261.

[41] G.R. Desiraju, T. Steiner, The Weak Hydrogen Bond: In Structural Chemistry and Biology, Oxford University Press1999.

[42] S. Itoh, Chemical Reactivity of Copper Active-Oxygen Complexes, Copper-Oxygen Chemistry, John Wiley & Sons, Inc.2011, pp. 225-282.

[43] K. Fagnou, M. Lautens, Halide Effects in Transition Metal Catalysis, Angew. Chem., Int. Ed., 41 (2002) 26-47.

[44] J.M. Berg, J.L. Tymoczko, L. Stryer, Biochemistry, Fifth Edition: International Version, W. H. Freeman2002.

[45] S. Stoll, A. Schweiger, EasySpin, a comprehensive software package for spectral simulation and analysis in EPR, J. Magn. Reson., 178 (2006) 42-55.

[46] G. Sheldrick, A short history of SHELX, Acta Crystallographica, Section A: Foundations of Crystallography, 64 (2008) 112-122.

Highlights:

Reaction of a coordinating cryptand with copper(II) chloride and fluoride leads to cryptates with different geometries. Only the C_3-symmetric fluoride reacts under oxidative conditions, illustrating a biologically relevant anion effect.

Graphical Abstract: